

Stabilization of Neoclassical Tearing Mode by Electron Cyclotron Current Drive and Its Evolution Simulation on JT-60U Tokamak

K. Nagasaki 1), A. Isayama 2), N. Hayashi 2), T. Ozeki 2), M. Takechi 2), N. Oyama 2), S. Ide 2), S. Yamamoto 1) and JT-60 Team

1) Institute of Advanced Energy, Kyoto University, Gokasho, Uji, Kyoto, Japan

2) Japan Atomic Energy Research Institute, Naka, Ibaraki, Japan

E-mail contact of main author: nagasaki@iae.kyoto-u.ac.jp

Abstract. Stabilization of an $m=3/n=2$ neoclassical tearing mode (NTM) by a local electron cyclotron current drive (ECCD) has been studied in the JT-60U tokamak. In the stabilization experiment, the EC injection timing is scanned from the “before mode onset” phase to the mode saturation phase. We have demonstrated that the ECCD is more effective when it is applied before the mode onset, and the critical timing for effective ECCD is related to the mode excitation phase. An ELMy H-mode plasma of $\beta_N=2.9$ has been sustained for 5 sec by suppressing the $3/2$ NTM using the second harmonic X-mode ECCD of 2.4 MW. A numerical study has been made on the basis of the modified Rutherford equation coupled with a 1.5D transport code and an EC code. The simulation well reproduces the time evolution of the magnetic island both at the growing and stabilizing phases. In the early ECCD, the changes in the background profiles such as the bootstrap current and/or the classical tearing parameter are required to explain the decrease of the mode amplitude.

1. Introduction

Neoclassical tearing mode (NTM) limits a plasma beta in present and future large tokamaks, since it appears before reaching ideal beta limit. Suppression of the NTM is an important task for sustaining high β plasmas stably. A localized current by an electron cyclotron wave (ECCD) is considered one of attractive methods to stabilize the NTM, which compensates the missing bootstrap current in the magnetic island. The $m=3/n=2$ NTM stabilization by unmodulated co-ECCD has been demonstrated experimentally in JT-60U [1, 2], AUG [3] and DIII-D [4]. Here m and n are poloidal and toroidal mode numbers, respectively. It has also been reported in DIII-D [5] and AUG [6] that the $2/1$ NTM is suppressed by using co-ECCD. In JT-60U, the $3/2$ NTM can completely be stabilized by applying the fundamental O-mode ECCD onto the center of the magnetic island. The EC current position is controlled in real time by detecting the magnetic island position from the electron temperature perturbation position. In International Thermonuclear Experimental Reactor, ITER, a 170GHz fundamental EC system is planned for the NTM stabilization in order to obtain high β performance [7].

The ECCD before the mode onset (early ECCD) has a potential to reduce the necessary EC power and to keep high plasma by avoiding the NTM excitation. In JT-60U, it has been reported that the early ECCD is more effective than the ECCD after the mode saturation (late ECCD) [8]. The mode amplitude is more suppressed at the same EC power, and the EC power for complete stabilization is lower. There are two equilibrium states at the same input power under the existence of the magnetic island, suggesting that there are nonlinear properties in the stabilization physics as well as the NTM excitation. A numerical simulation code has been developed to analyze the NTM behavior for JT-60U, in which the modified Rutherford equation is coupled with a 1.5D transport code and an EC code [9]. Undetermined parameters in the modified Rutherford equation are estimated by fitting to the experimental results [10].

The movement of the rational surface by ECCD is taken into account in the simulation. In this paper, we present the experimental and theoretical studies on the stabilization of the 3/2 NTM in JT-60U. In Sec. 2, shown are the experimental results on the early ECCD by fundamental ECCD and the sustainment of high β_N plasma by second harmonic ECCD. The numerical simulation using the modified Rutherford equation coupled with the 1.5D transport code and the EC code are shown in Sec. 3. The conclusion is given in Sec. 4.

2. NTM Stabilization Experiments by ECCD

2.1 Dependence of NTM on EC Injection Timing

The NTM is destabilized when the bootstrap current is reduced at the rational surface due to a local decrease of the pressure gradient in the magnetic island. Some tearing modes in high β_p H-mode discharge on JT-60U have the characteristics of the NTM; (1) the mode appears at high β , (2) there exists hysteresis characteristics in β value, that is, β value at the appearance is a few times higher than that at the disappearance, and (3) the modes such as $m/n=3/2$, $4/3$, $5/3$ and $2/1$ are excited at the rational surfaces where the pressure gradient is high. The magnetic island structure is formed at the rational surface once the NTM is excited. The island structure is measured with an ECE diagnostic using heterodyne radiometer. The spatial resolution is 1 cm, which is smaller than the saturated magnetic island width, 9 cm ($W/a \sim 0.1$, where W and a are the island width and the plasma radius, respectively). A flat region is formed in the T_e profile at $q=3/2$ when the 3/2 NTM is excited. The 110GHz ECH/ECCD system is used for the NTM stabilization with total injection power of 3 MW. The EC power is unmodulated, and the waves are launched with the finite toroidal injection angle so as to drive the non-inductive current in the co-direction of plasma current. The driven current density profile has a FWHM of $\Delta\rho=0.06$. The fraction of the EC driven current to the total current is about 5 %.

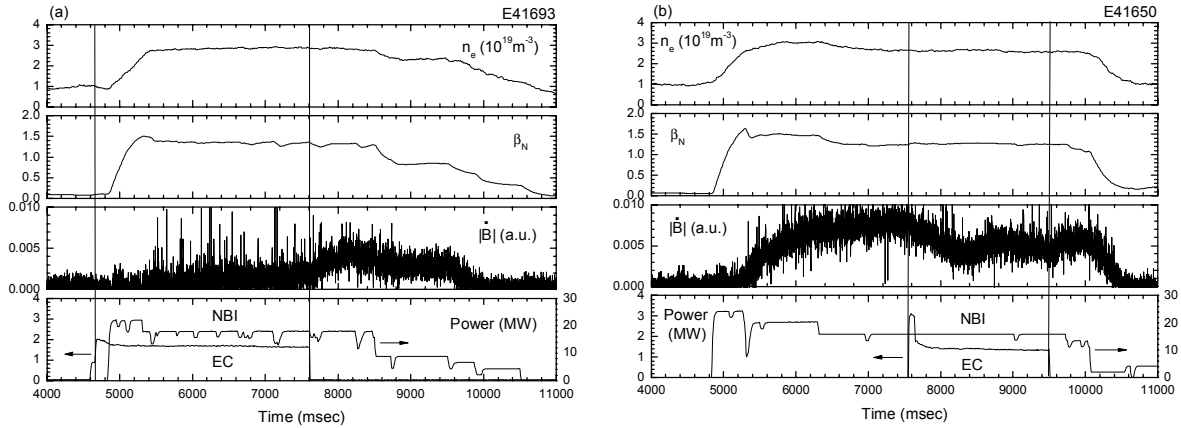


Fig. 1 Time evolution of 3/2 NTM stabilization in ELMy H-mode plasma. The fundamental ECCD is applied (a) before the mode onset and (b) after the mode onset.

Figure 1 shows the example of the time evolution in the ECCD stabilization experiment. The plasma parameters are $I_p=1.5$ MA, $B_t=3.66$ T, $R=3.3$ m, $a=0.9$ m and $q_{95}=3.8$. After the NB injection of 20 MW power, the plasma enters into a high β_p ELMy H-mode state, where the averaged electron density is $3.0 \times 10^{19} \text{ m}^{-3}$ and the central electron temperature is 6 keV. When β_N reached around 1.4, the 3/2 mode is destabilized and the magnetic fluctuation is enhanced, which is measured with saddle and Mirnov coils. The NB power is controlled so as to keep β_N

as 1.4 in order to investigate the stabilization effect on the 3/2 mode, where the 3/2 mode appears reproductively without the 2/1 mode excited. The mode frequency is not changed so much within the range of 10-12 kHz regardless of the EC injection. The injection timing is changed from the “before onset” phase to the saturation phase in order to study the response of the NTM. The injected EC power is 1.7 MW. According to the Fokker-Planck code and the ACCOME code, the total EC driven current is about 43 kA, and its peak current density is 0.17 MA/m² under the experimental conditions, which is a little lower than the bootstrap current density. The EC current location is fixed in the early ECCD, while it is real-time controlled by detecting the mode location in the late ECCD. The $q=3/2$ surface moves during the discharge, but its shift is not large, $\Delta\rho\sim 0.01$. In the late ECCD, the EC current position is finely tuned by evaluating the standard deviation of the T_e perturbation profile. In the early ECCD, the 3/2 NTM is almost stabilized, while the fluctuation level is higher in the late ECCD. The EC power for complete stabilization is 20 % lower when it is applied before the mode onset. The time delay of the mode onset from the NB turn-on becomes long with an increase of the EC power. Thus the early ECCD is found to be more effective than the late ECCD. The hysteresis characteristics exist in the ECCD stabilization as well as the NTM excitation. The stabilization effect is sensitive to the EC current position. The 3/2 NTM is not suppressed well as the EC current position deviates from the $q=3/2$ surface by half of the EC current width.

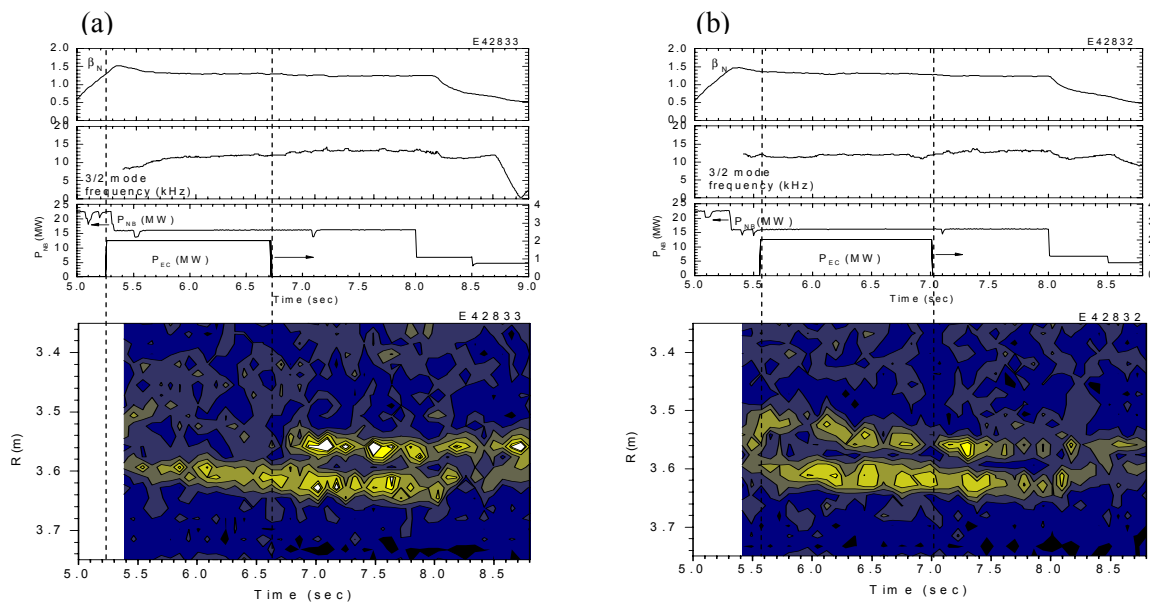


Fig. 2 Time evolution of perturbed T_e contours around $q=3/2$ surface. The fundamental ECCD is applied (a) before the mode onset and (b) after the mode onset. The power and position of applied EC are fixed as $P_{EC}=2.1\text{MW}$ and $\rho_{EC}=0.5$.

The shrinkage of the magnetic island structure during the early ECCD is asymmetric in the radial direction. Figure 2 shows the time evolution of perturbed T_e contours around the $q=3/2$ surface. In this scanning experiment, the EC current position is deviated from the island center by 7 cm. Nevertheless the effect on the island structure can be investigated. The mode amplitude at the high field side (inner half of the island) decreases, while it does not at the low field side (outer half of the island). This tendency was also observed when the NTM was completely stabilized by real time controlled ECCD at the mode saturation phase [2]. The magnetic island at the inner region starts to grow when ECCD is turned off. Figure 3 shows the dependence of T_e perturbed region on the EC injection timing. The inner and outer widths of T_e perturbed region is estimated by the perturbed T_e contours around the $q=3/2$ rational surface. Note that this perturbed region may reflect the island structure, but the width is about

twice as the island width determined by the separatrix of flux surface. The T_e perturbation at the inner region is strongly dependent on the EC injection timing. It does not appear when the EC power is applied prior to the mode onset. On the other hand, at the outer region, it decreases as the EC injection timing is earlier, but its change is modest. The critical timing for effective ECCD is related to the mode onset phase. The application of ECCD at the NTM onset is not as effective as the before-onset phase. This may indicate that the early ECCD should be applied before detecting the NTM in order to make the necessary EC power lower.

The time evolution of current profile associated with magnetic island formation is measured with a Motional Stark Effect (MSE) spectroscopy. As the magnetic island is formed at the rational surface, the current is decreased and its profile is flattened at the radial location of the magnetic island structure. For the 3/2 NTM stabilization experiment, an increase in current density is observed during the ECCD on, and the flat region disappears when the 3/2 mode is completely suppressed. The detail of current profile measurement is described in Ref. [11].

2.2 Sustainment of High β_N Plasma using Second Harmonic ECCD

The ECCD stabilization experiment at higher β_N has been performed using the second harmonic co-ECCD at an ELMy H-mode plasma of $I_p = 0.85$ MA, $B_t = 1.7$ T, and $q_{95} = 3.5$. The EC injection position and the magnetic field are fixed in this experiment. According to the EC ray tracing code and the ACCOME code, the maximum EC current density, $J_{EC} = 0.20$ MW/m², is comparable to the bootstrap current density at $q = 3/2$. The absorbed EC power is 2.4 MW, and the FWHM of the EC current profile is 0.10. Figure 4 shows the time evolution of the ECCD stabilizations in two different EC current position cases. In the successful stabilization, the EC current is located at $\rho_{EC} = 0.50$, which may be closer to the $q = 3/2$ surface. β_N is kept high ~ 2.9 by feedback control of NB power. The input power amount is decreased at $t = 7.6$ - 7.9 sec, indicating that the energy confinement is improved. Although the suppression of 3/2 NTM is not as clear as in the fundamental ECCD, a high confinement plasma of $\beta_p \sim 1.7$, $H_{89PL} \sim 1.8$, $\beta_N \sim 2.9$, $H_{89PL}\beta_N \geq 5$ can be sustained for 5 sec. The discharge is terminated by a major disruption at $t = 8.8$ sec, whose cause should be made clear in the future. When the EC current is deviated by $\Delta\rho_{EC} = 0.02$, the mode amplitude is less reduced, and β_N and the neutron production rate continue to decrease. As the EC power is lower, the 2/1 and 5/3 NTMs are excited, resulting that the degradation of β_N cannot be recovered by ECCD. The excitation of 2/1 NTM may be related to the 3/2 NTM amplitude. The suppression of 3/2 NTM or the modification of the T_e and/or current profile may affect the appearance of 2/1 NTM.

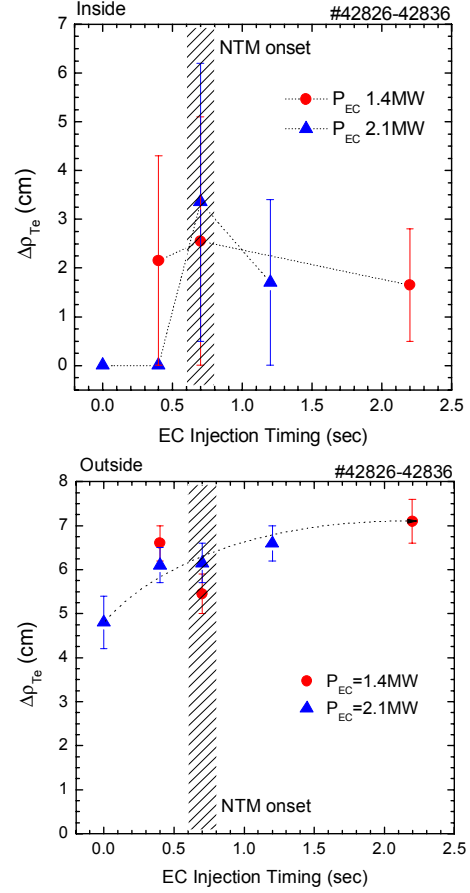


Fig. 3 Dependence of T_e perturbation width on EC injection timing, (a) inner width and (b) outer width.

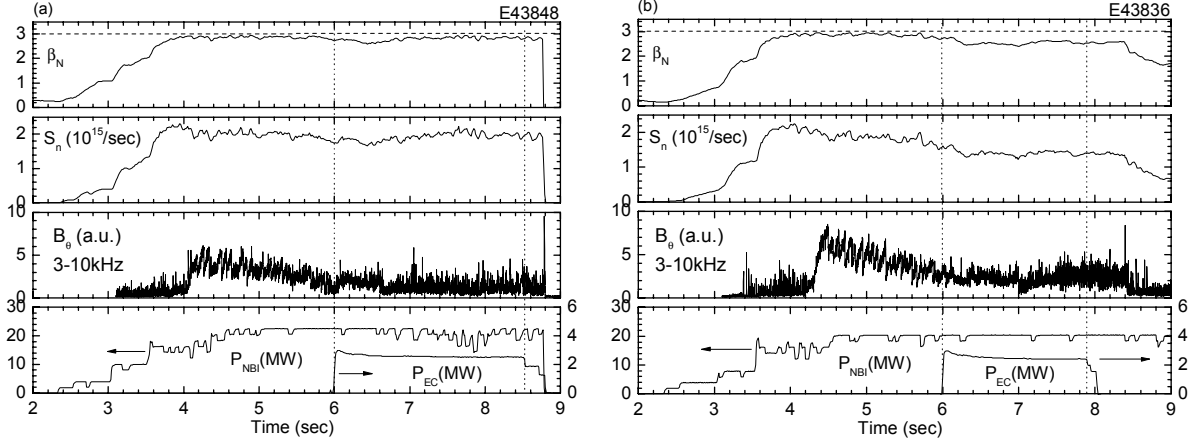


Fig. 4 Time evolution of 3/2 NTM stabilization in $\beta_N=2.9$ ELMy H-mode plasma. The EC power of 2.4 MW (EC current of 57 kA) is applied at (a) $\rho_{EC}/a=0.50$ and (b) $\rho_{EC}/a=0.54$. The high performance plasma of $\beta_p \sim 1.7$, $H_{89PL} \sim 1.8$, $H_{89PL}\beta_N \geq 5$ is sustained for 5 sec at $\rho_{EC}/a=0.50$.

3. Simulation of NTM Stabilization

3.1 Numerical Model

The time evolution of an $m/n=3/2$ NTM and its stabilization by ECCD are investigated by using a numerical model. The time evolution of the magnetic island is calculated by the modified Rutherford equation coupled with the 1.5D transport code [9][10][12]. The transport code self-consistently solves the 1D transport and current diffusion equations, and the Grad-Shafranov equation of the MHD equilibrium in the 2D plane without the island structure. In order to take account of the background current profile modification by the EC current, the current diffusion equation is calculated in the 1.5D transport code. It should be noted that the modification of pressure and current profiles due to the island formation is not considered. The time evolution of an NTM island full-width, W , is given by the following modified Rutherford equation,

$$\frac{dW}{dt} = k_c F_{\Delta'} + k_{BS} F_{BS} + k_{GGJ} F_{GGJ} + k_{pol} F_{pol} + k_{EC} F_{EC} \quad (1)$$

where $k_c F_{\Delta'}$, $k_{BS} F_{BS}$, $k_{GGJ} F_{GGJ}$, $k_{pol} F_{pol}$ and $k_{EC} F_{EC}$ represent the contributions from the equilibrium current profile, the bootstrap current, the toroidal geometry (called Glasser-Green-Johnson effect), the ion polarization current, and the EC current, respectively. The coefficient, k_c , is chosen as $k_c = 1.2$, and the tearing parameter, Δ' , is calculated by a cylindrical model. The function, F_{BS} , includes a characteristic island width, W_d , due to the effect of the parallel and perpendicular heat transport. The localization efficiency of EC current is calculated numerically according to the EC current profile on the flux surface of an island structure. The coefficients, k_{BS} , k_{GGJ} , k_{pol} , k_{EC} and W_d , in Eqn. (1) are estimated by comparing with experiments since it is hard to determine them accurately from the theory. The coefficient, k_{BS} can be estimated from the saturation phase since the saturation is almost determined by $F_{\Delta'}$ and F_{BS} . The other parameters of k_{GGJ} , k_{pol} and W_d can be estimated when the island is small, since the small island behavior much depends on them.

3.2 Calculation Results and Comparison with Experiment

Numerical results are compared with JT-60U experiments in order to validate the numerical model. Two discharges in JT-60 experiments are selected, i.e., one is related to the NTM

island growth (E36705) and the other is the stabilization by the real-time control of ECCD (E41666). An $m/n=3/2$ mode NTM is destabilized at $\beta_N=2$ for E36705 and 1.5 for E41666 by the NB injection of 20 MW. The experimental island width is evaluated by using the T_e perturbation profile measured with the ECE and the magnetic fluctuation amplitude under the assumption that the island width is proportional to the square root of the magnetic fluctuation amplitude in the cylindrical model. The numerical result strongly depends on k_{BS} , and they are best fitted to the experimental data when $k_{BS}\sim 5$, while the island width is weakly dependent on k_{GGJ} and k_{pol} . The characteristic island width is estimated as $W_d=0.008$ in the growing phase, which is close to the flux-limit model. In the stabilization phase, on the other hand, the coefficients are estimated as $k_{BS}=4.5$, $k_{GGJ}=k_{pol}=1$ and $W_d=0.02$. This characteristic island width also agrees with the flux-limit model. If the misalignment of the EC current position, $\Delta\rho=\rho_{EC}-\rho_s$, is considered, the experimental value is well fitted to the numerical results at $(\Delta\rho, k_{EC})=(0.0, 3.0)$, $(0.025, 3.4)$ and $(-0.025, 4)$. This misalignment is within the range of the experiment. Figure 5 shows the time evolution of the magnetic island width at the growing and stabilization phases. The numerical model well reproduces the JT-60U experimental results for a set of parameters in the modified Rutherford equation. The estimated parameters are not inconsistent between two discharges.

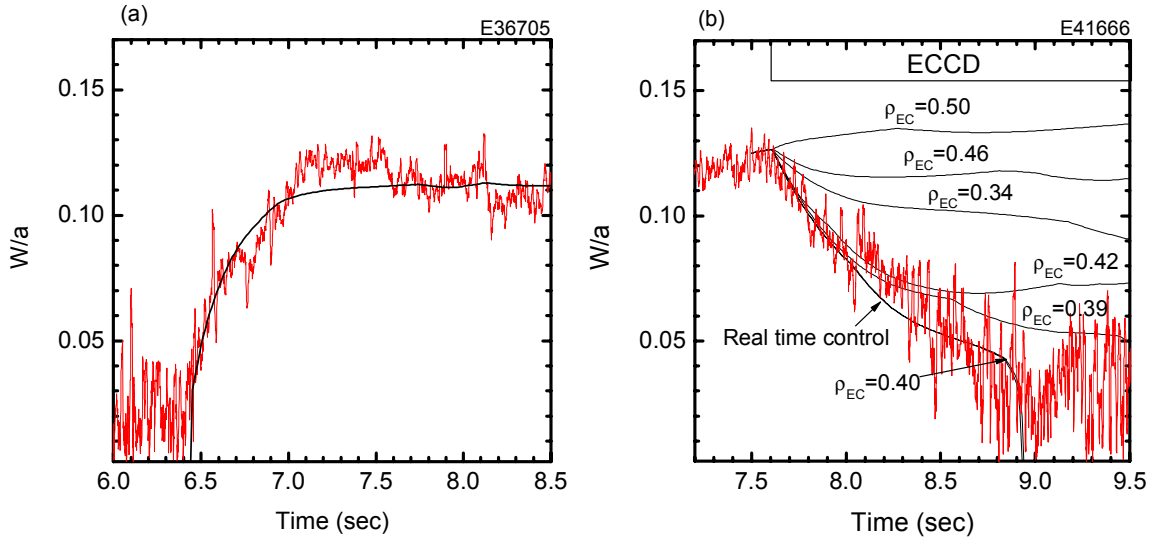


Fig. 5 Time evolution of magnetic island width in JT-60U plasma, (a) growing phase and (b) stabilizing phases. The red and black lines denote the experimental and simulation results, respectively.

Following the determination of the coefficients in the modified Rutherford equation, we have compared the dependencies on the EC power and the EC current position between the experimental and simulation results. Figure 6 shows the dependence of the magnetic island width on the EC power. In the stabilization experiment by late ECCD, a real time EC control is performed to adjust the EC current position. On the other hand, the EC current position is fixed at the initial $q=3/2$ surface in the early ECCD. In the experiment, the saturated island width is different between the early and late ECCD. The island in the early ECCD is smaller than in the late ECCD, and the EC power for complete suppression is lower. The island width in the late ECCD agrees well with the simulation, while it is much smaller in the early ECCD. The reduction of the power threshold for complete stabilization can be explained by the simulation, because the seed island for the mode excitation becomes large as the EC power is increased. However, in the simulation, once the mode is excited, the final mode amplitude is not changed regardless of the EC injection timing.

An additional stabilizing effect of the early ECCD could give from making the background plasma parameters changed. The island becomes small if the stabilizing terms such as the tearing parameter are more negative, or the destabilizing terms such as the bootstrap current contribution are less positive. The function F in the modified Rutherford equation is re-estimated in order to explain the experimental mode amplitude. We assume that only one term is changed so that the calculated mode amplitude can be equal to the experimental result. Table 1 shows the ratio of the function value in the early ECCD to that in the late ECCD. In the saturation phase, the island width is mainly determined by the bootstrap current, the classical tearing parameter and the ECCD. The polarization and GGJ terms are negligible since they are too small to explain the change in dW/dt at the mode saturation phase. The ECCD term may be almost unchanged. As can be seen in Table 1, the estimated change in the bootstrap current term seems reasonable. The classical tearing parameter may also be more negative, contributing to the stabilization. The background profiles are possibly different between the early and late ECCD, leading that the function values, F_{BS} and/or F_{Δ} , are changed. This situation is maintained during the mode evolution.

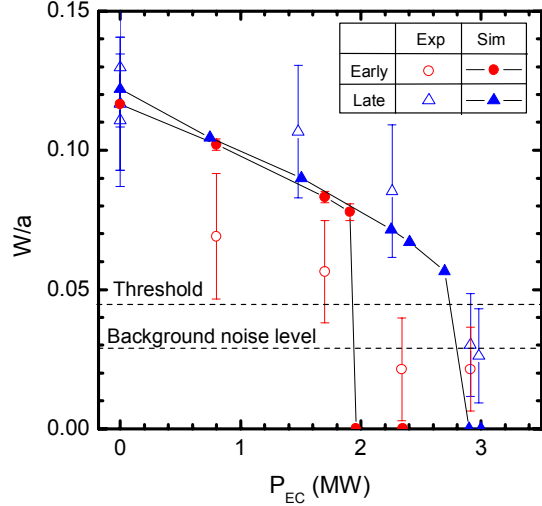


Fig. 6 Comparison of magnetic island width between experimental and simulation results.

	Bootstrap current term	Classical tearing term
$P_{EC}=0.8$ MW ($I_{EC}=20$ kA)	0.63	2.17
$P_{EC}=1.7$ MW ($I_{EC}=43$ kA)	0.77	1.71

Table 1 Estimated ratio of the MRE function value in early ECCD to that in late ECCD.

The stabilization effect is sensitive to the position of the EC driven current also in the early ECCD. The precise adjustment of the power deposition is required to achieve the effective stabilization. The ECCD is well localized within the region of $\Delta\rho=0.12$, which is comparable to the saturated island width. The simulation results indicate that the mode is not suppressed well if the position of the EC driven current is deviated from the $q=3/2$ rational surface by half of the EC current width. When the power absorption position is shifted outwardly from the optimum position, the mode is reduced but gradually increases during the EC pulse duration. This tendency is qualitatively in agreement with the experimental results.

4. Conclusions

The stabilization of $m=3/n=2$ NTM has been studied in high β_p ELMy H-mode plasmas on the JT-60U tokamak. The ELMy H-mode plasma with $q(0)>1$ and no NTM give a high performance scenario in future burning plasma experiments such as ITER. The ECCD before the mode onset is more effective than that at the saturation phase, and the critical EC timing for effective ECCD is associated with the mode onset phase. The early ECCD is less effective

even just after the mode excitation. The ECE measurement indicates that T_e perturbation decays asymmetrically in the radial direction. The high β_p ELMy H-mode plasma of $\beta_N=2.9$ has been sustained by 2.4MW second harmonic ECCD for 5 sec. The 3/2 NTM is suppressed and the 2/1 NTM excitation can be avoided by controlling the EC current location precisely. A numerical study of the NTM stabilization by ECCD has been made on the basis of the modified Rutherford equation with 1.5D transport code and EC code. The simulation results well reproduce the time evolution of the 3/2 NTM experimentally observed both at the growing and stabilizing phases. In the experiment, there exist two equilibrium states with finite island structure at the same EC power condition. The mode amplitude can be explained by the simulation in the late ECCD case, while the change in the background plasma profiles such as the classical tearing parameter and/or the bootstrap current is required in the early ECCD case. The numerical calculation including the modification of background profiles will be performed in the future.

Acknowledgement

We would like to thank Drs. T. Takizuka, K. Hamamatsu, T. Suzuki and K. Kobayashi for fruitful discussions and supports. Authors thank JAERI staff for the JT-60U operation and useful discussions. One of the authors (K. N.) is grateful to the Heliotron J staff for continuous discussion. This work was carried out as a joint work under the Facility Utilization Program of JAERI.

References

- [1] ISAYAMA, A., et al., "Complete stabilization of a tearing mode in steady state high- β_p H-mode discharges by the first harmonic electron cyclotron heating/current drive on JT-60U", Plasma Phys. Control. Fusion 42 (2000) L37-L45.
- [2] ISAYAMA, A. et al., "Achievement of high fusion triple product, steady-state sustainment and real-time NTM stabilization in high- β_p ELMy H-mode discharges in JT-60U", Nucl. Fusion 43 (2003) 1272-1278.
- [3] GANTENBEIN, G. et al., "Complete Suppression of Neoclassical Tearing Modes with Current Drive at the Electron-Cyclotron-Resonance Frequency in ASDEX Upgrade Tokamak", Phys. Rev. Lett. 85 (2000) 1242-1245.
- [4] LA HAYE, R. J., "Control of neoclassical tearing modes in DIII-D", Phys. Plasmas 9 (2002) 2051-2060.
- [5] PETTY, C. C., "Complete suppression of the $m = 2/n = 1$ neoclassical tearing mode using electron cyclotron current drive in DIII-D", Nucl. Fusion 44 (2004) 243-251.
- [6] GANTENBEIN, G. et al., "Investigations on $m=2, n=1$ Tearing Mode Stabilization with ECRH at ASDEX Upgrade", Proc. European Conf. on Control. Fusion and Plasma Physics (St. Petersburg, 2003) Vol. 27A, P-1.187-191.
- [7] ITER Physics Expert Group on Energetic Particles, Heating and Drive and ITER Physics Basis Editors, Nucl. Fusion 39 (1999) 2495-2540.
- [8] NAGASAKI, K., et al., "Stabilization effect of early ECCD on a neoclassical tearing mode in the JT-60U tokamak", Nucl. Fusion 43 (2003) L1-L4.
- [9] HAYASHI, N., et al., "ECCD power necessary for the neoclassical tearing mode stabilization in ITER", Nucl. Fusion 44 (2004) 477-487.
- [10] HAYASHI, N., "Numerical Analysis of Neoclassical Tearing Mode Stabilization by Electron Cyclotron Current Drive", J. Plasma Fusion Res. 80 (2004) 605-613.
- [11] OIKAWA, S., this conference, EXP/5-15
- [12] HAYASHI, N., et al., "Simulation on Neoclassical Tearing Mode Stabilization by ECCD for JT-60 Superconducting Tokamak", J. Plasma Fusion Res. SERIES, 5 (2002) 519-522.